

Heavy Neutrino Searches via Same-sign Lepton Pairs at the Higgs Factory

Yu Gao^{1*} and Kechen Wang^{2†}

¹ *Key Laboratory of Particle Astrophysics, Institute of High Energy Physics,
Chinese Academy of Sciences, Beijing, 100049, China and*

² *Department of Physics, School of Science, Wuhan University of Technology, 430070 Wuhan, Hubei, China*

This paper investigates the $e^+e^- \rightarrow Zh$ sensitivity for Higgs boson's rare decay into heavy neutrinos $h \rightarrow NN$ at the proposed electron-positron collider, with the focus on multi-lepton final states that contain same-sign lepton pairs. $h \rightarrow NN$ decay can derive from Higgs boson's mixing with new physics scalar(s) that is complementary to the contribution from active-sterile neutrino mixings. We analyze the semileptonic, fully leptonic and mixed NN decay scenarios, and categorize the signal on the number of leptons in the final state: $\ell^\pm\ell^\pm$ with at least 3 jets, $\ell^\pm\ell^\pm\ell$ with at least 2 jets, and $e^\pm e^\pm \mu^\mp \mu^\mp$ plus with at least 1 jet, each containing one or two same-sign dilepton system(s). Selection cuts are optimized for the presence of the associated Z boson, which leads to additional backgrounds at the e^+e^- collider. The Standard Model background channels are systematically analyzed. Sensitivity limits on $h \rightarrow NN$ branching fractions are derived for signals with 2-4 final leptons assuming the heavy neutrino masses are between 10 and 60 GeV. With 240 GeV center-of-mass energy and 5.6 ab^{-1} design luminosity, $h \rightarrow NN$ branching fraction can be probed to 2×10^{-4} in 2ℓ and 3ℓ channels, and 6×10^{-4} in the 4ℓ channel at 95% credence level. $3\ell, 4\ell$ channels expect one or fewer background event, and their sensitivities saturate the statistic limit at 5.6 ab^{-1} luminosity. A same-sign *trilepton* ($\ell^\pm\ell^\pm\ell^\pm$) signal in the 3ℓ channel is also discussed.

I. INTRODUCTION

The collider search for massive neutrinos plays an important role in the testing of neutrino mass models that base on the seesaw mechanism [1–5]. Mass of the active neutrino ν is generated by mixing the left-handed neutrino (ν_L) of the Standard Model (SM) with the additional right-handed neutrino N_R , resulting in a heavy mass eigenstate N that has a small SM ν_L component. The heavy N acquires effective couplings to the SM model gauge bosons via its weakly charged ν_L component [6] and is extensively searched at colliders. See Ref. [7–9] for recent experimental limits.

While the heavy N_R mass scale explains the tiny active neutrino mass, it also suppresses the left-right neutrino mixing, and makes weak production of heavy neutrinos difficult when this mixing is small. Alternatively, heavy neutrinos can also be produced in case they couple to Beyond the Standard Model (BSM) mediators, e.g. extra gauge bosons or scalars that couple to SM particles. Currently, such BSM gauge bosons are stringently constrained by resonance searches [10, 11] and electroweak precision data [12, 13]. In comparison, a mixing between the Higgs boson with BSM singlet scalar(s) is less constrained [14], and it is among the major physics goals at future Higgs factories [15, 16].

The right-handed neutrino can obtain its mass by coupling to BSM scalars with a non-zero vacuum expectation value (vev). Generally such scalars mix with the SM Higgs doublet scalar, so if kinematically allowed, the physical Higgs boson can decay into heavy neutrinos through its BSM component. Since this decay oc-

curs directly through the scalar mixing, it is insensitive to $\nu_L - N_R$ mixing, thus it is complementary to $|V_{\ell N}|^2$ based searches. Typical implementations involve extending the SM's scalar sector, e.g. from UV-complete models such as left-right symmetric models [17], $U(1)_{B-L}$ models [3], next to minimal supersymmetric model [18], or alternatively, rising from effective theory operators [19], 4th generation neutrino [20], etc.

When the Higgs boson decay into heavy neutrinos $h \rightarrow NN$, a rare multi-lepton Higgs decay emerges. N subsequently decays to SM particles through its ν_L component's weak interaction. The fully leptonic $N \rightarrow \ell\ell'\bar{\nu}$ and semileptonic $N \rightarrow \ell jj$ channels are interesting at collider searches due to the presence of measurable charged leptons in the final state. When N is a Majorana fermion, semileptonic NN decay leads to the characteristic lepton-number violating (LNV) same-sign (SS) dilepton, as recently studied as a LNV probe for Higgs-BSM scalar mixing [21–24]. Fully leptonic NN decay allows up to two pairs of same-sign same-flavor (SSSF) dileptons for either Majorana or Dirac N [25].

For collider searches, increased lepton multiplicity and the existence of SS lepton pairs greatly reduce the SM's contamination, particularly for hadron collisions. At lepton colliders, in comparison, hadronic backgrounds are controllable and the dominant Higgs boson production is the $e^+e^- \rightarrow hZ$ channel. An associated Z boson always appears and it provides additional lepton or jets to the final state. Thus it is of interest to study the multi-lepton sensitivity at future lepton colliders.

The proposed lepton collider missions, e.g. the CEPC [26], ILC [27] and FCC-ee [28], are designed to yield $\mathcal{O}(10^{6-7})$ Higgs events. Any Higgs decay branching limit would be statistically capped by the collider's luminosity-inverse. Study on the relevant backgrounds would help understanding whether future $h \rightarrow NN$ sen-

* gaoyu@ihep.ac.cn

† kechen.wang@whut.edu.cn

sensitivity would saturate luminosity limits.

This paper is organized as follows: Section II briefly discusses a minimal singlet extension to the SM that implements the $h \rightarrow NN$ decay channel. Section III to V categorize signal channels on the number of final state leptons, analyze each channel's SM background and the event selection strategies. In Section VI we give the sensitivity limits at future Higgs factory.

II. MODEL SETUP

For collider search purposes, we adopt the minimal effective extension to the Standard Model that implements a Type-I seesaw mechanism. With a scalar S and Majorana fermion N_R that are both SM gauge singlets, the addition to interaction Lagrangian is given by,

$$\Delta\mathcal{L} \supset y_D \bar{L} H N_R + y_S S N_R N_R + c.c. + \lambda |H|^2 |S|^2 + V_S. \quad (1)$$

where y_D and y_S are the couplings that give the Dirac and Majorana mass terms after the SM Higgs doublet H and the singlet S obtain vacuum expectation values. The new scalar potential involves H, S mixing term and S self-interacting terms. We would also assume a small mixing term $\lambda v_S v_H \ll m_h^2$, so that V_S minimization does not qualitatively impact the SM electroweak sector. The scalars then mix by a small angle α ,

$$\begin{pmatrix} h_1 \\ h_2 \end{pmatrix} = \begin{pmatrix} \cos \alpha & -\sin \alpha \\ \sin \alpha & \cos \alpha \end{pmatrix} \begin{pmatrix} h \\ s \end{pmatrix}. \quad (2)$$

where h, s represent the Higgs doublet and singlet modes around their vevs. h_1, h_2 are the physical mass eigenstates. h_1 is dominated by h and it identifies with the 125 GeV boson. h_2 is singlet s dominated, and it picks up a weakly charged h component via mixing. h_2 is subject to diphoton resonance searches [29, 30] and its mass range is less stringently constrained when the mixing angle is small,

$$\alpha = \frac{\lambda v_H v_S}{|m_s^2 - m_h^2|}, \quad (3)$$

where m_s and m_h are the singlet and Higgs doublet masses. In the small-mixing limit ($\lambda \rightarrow 0$), the denominator can be well approximated by $|m_s^2 - m_h^2| \sim |m_{h_1}^2 - m_{h_2}^2 + \mathcal{O}(\sin^2 \alpha)|$ if the scalars are not mass-degenerate. Interestingly, if h_2 resides in the mass window $2m_N < m_{h_2} < E_{\text{COM}} - m_Z$, production of $Z h_2$ is kinematically viable and $h_2 \rightarrow NN$ decay can also contribute significantly to the signal. However, it would also require m_{h_2} to be comparable to the Higgs boson's mass when the center-of-mass energy E_{COM} is limited, particularly so if the e^+e^- energy is just above the Zh threshold at the Higgs factory. In this work, we assume m_S to be generally heavier than this mass window and focus on h_1 production. We also assume $m_N < m_{h_1}/2$ so that the

$h_1 \rightarrow NN$ is not further virtuality-suppressed. Note that a very light singlet scalar scenario $m_S \ll m_H$ is possible: it requires a shallow $V(S)$ potential with v_S above the weak scale, so that $m_{N_R} \sim y_N v_S$ with $y_N \leq \mathcal{O}(1)$ still gives a massive N heavy enough to decay inside the detectors.

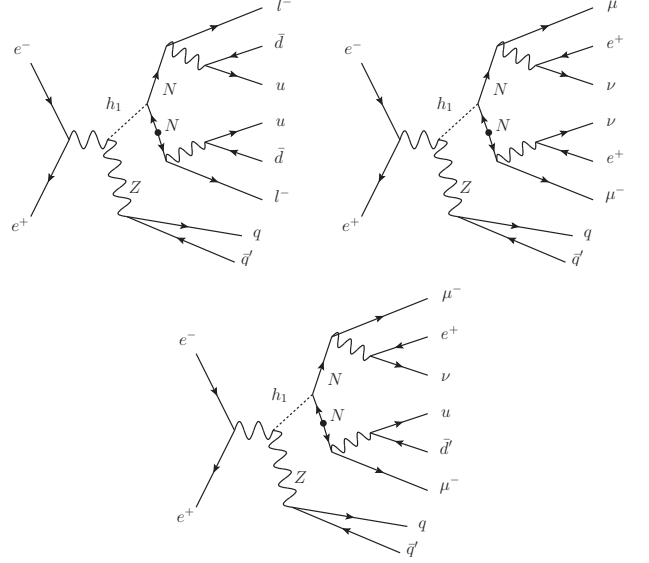


FIG. 1. Illustrative processes of SS dilepton production from semileptonic (upper left), leptonic (upper right) and mixed (lower) decays of the NN system. Note the leptonic and mixed decay scenarios also produce SS dileptons without LNV [25].

Unlike Higgs production in pp collision where gluon fusion dominates, the leading production channel in e^+e^- collision is through the s -channel Z with an associated final state Z boson, as shown in Fig. 1. The $h_1 \rightarrow NN$ system leads to the characteristic rare Higgs decay signals with SS lepton pair(s). Here we do not include the $h(Z) \rightarrow N\nu$ decays [31–35] as their branching fractions rely on $|V_{\ell N}|^2$. The Z boson can decay to a lepton or jet pair and their invariant mass reconstructs to m_Z . For signal selection, visible decays of the Z boson are favorable as they would:

(i) demand SM background to be also accompanied by one additional Z boson;

(ii) remove potential lepton number uncertainty from neutrinos in case LFV is required in the final state.

The $h_1 \rightarrow NN$ branching fraction is proportional to $\sin^2 \alpha$. N decays through its ν_L component thus its decay width is $|V_{\ell N}|^2$ suppressed. $N \rightarrow \ell W^*$ is the dominant N decay channel, its hadronic and leptonic $W^* \rightarrow jj, \ell\nu$ decays lead to ‘semileptonic’ and ‘fully-leptonic’ final states, see [25] for branching fraction calculations. The $N \rightarrow \nu h^*, \nu Z^*$ channels are subleading and they require missing or wrong-sign leptons to form SS dileptons.

A major SM background consists of τ -lepton or on-shell W boson decays, where the $W\ell\nu$ vertex can couple

to any lepton flavor. Same-sign and same-flavor dilepton requires the presence of same-sign τ or W pairs, and charge conservation would demand four $W^{(*)}\ell\nu$ vertices in a SM final state. Same-sign, different-flavor dileptons arise from lepton pair production from neutral bosons, which can be vetoed by lepton flavor cuts. Another background arises from wrong-sign leptons or missed leptons that can be controlled by stringent lepton cuts in event analysis. The following sections will discuss the backgrounds for each channel.

In a final state with three or more leptons, opposite-sign same-flavor (OSSF) lepton pairs should be vetoed to suppress the SM background, which also means at least one SSSF lepton pair will be selected. For some signal processes this requires N to couple to more than one lepton flavor, and we would assume N couples equally to both e and μ flavors in our analysis.

We perform cut-and-count analyses on Monte-Carlo simulated signal and background events. Events are generated by MadGraph5 [36] and showered by Pythia8 [37, 38] package. τ lepton decays are handled by TAUOLA [39] as is implemented in Pythia8. e^-e^+ detector simulation is performed by DELPHES [40] with CEPC parametrization [41]. At event generation level we adopt jet cuts $\eta(j) < 5.0$, $p_T(j) > 20$ GeV and use relatively lenient lepton cuts $\eta(\ell) < 2.5$, $p_T(\ell) > 0.5$ GeV. Angular separation cuts $\Delta R(j, j)$, $\Delta R(\ell, \ell) > 0.3$ are also implemented.

III. TWO LEPTON CHANNEL

The $h_1 \rightarrow NN \rightarrow \ell^\pm\ell^\pm + 4j$, $\ell = e, \mu$ channel requires both N decay to a charged lepton and two jets ($W^* \rightarrow \bar{q}q'$) and one of the N s decays as its own antiparticle. This final state has no missing energy and violates lepton number with $\Delta L = 2$, and it is often considered the ‘smoking-gun’ channel of the heavy Majorana neutrino search with explicit LNV.

Note in this channel NN decays to four jets. Unlike being easily contaminated in pp collision [42, 43], the much cleaner environment in e^+e^- collision is largely free of fake leptons from soft jets. However, due to the small energy cap between the Higgs boson and heavy neutrino, these the four jets are relatively soft and can be difficult to fully reconstruct. With fewer jet counting, wrong-sign and unreconstructed leptons become possible backgrounds, in addition to intrinsic multiple- τ , W backgrounds. The relevant background channels are listed in Table I.

The background channels contain two or more τ leptons or light charged leptons $\ell = e, \mu$, plus Z or W^+W^- that yield dijet resonance near Z mass. The particle signs are omitted and any even number of τ, ℓ and W entries must include equal number of opposite-sign particles, e.g. 4τ denotes $2\tau^+2\tau^-$, and $2\ell 2W$ stands for $\ell^+\ell^-W^+W^-$, etc. While the SM backgrounds $\ell\ell$ are restricted to same-flavor, opposite sign lepton pairs, leptonic W decay can

provide one additional lepton and create a like-sign dilepton combination in case one lepton is un-detected. Such channels are marked with † in the table.

The signal event contains one SS dilepton, two jets from Z decay and a number of soft jets, plus very little missing energy. We select hadronic Z decay by imposing charged lepton number $N(\ell) = 2$ to avoid confusion between the leptons from Z decay and those from NN decay. With a jet transverse momentum requirement $p_T(j) > 20$ GeV the soft jets from the NN system are not always identifiable, especially when the jets are more collimated if N is light and relatively boosted. Still, having at least one extra jet in addition to those from Z can be effective in background rejection, so we consider the jet counting cut $N(j) \geq 3$.

Event selection includes the following cuts:

- (i) exactly two leptons, $N(\ell) = 2$ with $p_T(\ell) > 5$ GeV;
- (ii) two leptons have the same sign;
- (iii) veto τ leptons, $N(\tau) = 0$;
- (iv) at least three jets, $N(j) \geq 3$;
- (v) small missing energy, $\cancel{E}_T < 15$ GeV.

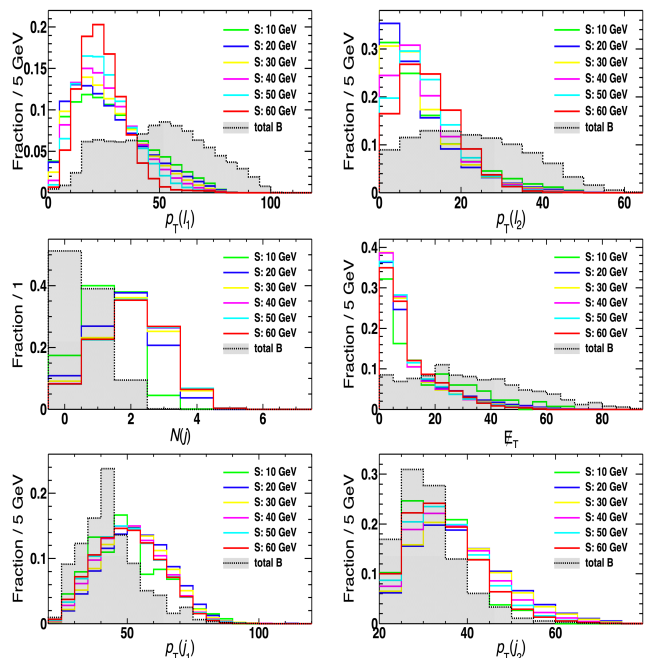


FIG. 2. Normalized distribution of selected kinematic variables to differentiate signals from the total SM background for the 2ℓ channel. $p_T(\ell)$ panels are after selecting $N(\ell) = 2$, $N(j)$ is after cut (ii), \cancel{E}_T , $p_T(j_2)$, $p_T(j_3)$ panels are after cut (iv).

The histograms of a few crucial kinetic observables for the signal with different m_N and the total background are shown in Fig. 2. $p_T(\ell_1)$ and $p_T(\ell_2)$ correspond to the samples after requiring $N(\ell) = 2$; $N(j)$ is after selecting cuts (i-ii); \cancel{E}_T , $p_T(j_2)$, $p_T(j_3)$ are after requiring cuts (i-iv). These distributions illustrate the effectiveness of our selection cuts. The $N(j)$ cut can be very effective in background rejection, and we select $N(j) \geq 3$ as it yields the best signal significance.

		initial	cuts(i-ii)	cuts(iii-iv)	cuts(v)
Sig.	10 GeV	10^3	6.3	0.29	0.18
	20 GeV	10^3	35.9	8.8	6.4
	30 GeV	10^3	72.3	22.6	17.5
	40 GeV	10^3	97.2	32.5	25.3
	50 GeV	10^3	112	37.4	28.8
	60 GeV	10^3	121	40.5	30.2
Bkg.	4τ	1.69×10^4	870	4.6×10^{-2}	7.7×10^{-3}
	$^\dagger 2\tau Z$	6.80×10^5	2.91×10^3	4.6	0.93
	$^\dagger 2\ell Z$	1.74×10^6	3.98×10^3	-	-
	$4\tau Z$	93.0	2.0	0.19	5.9×10^{-2}
	$2\tau 2W$	4.42×10^3	63.6	0.92	8.2×10^{-2}
	$^\dagger 2\ell 2\tau Z$	584	13.8	2.0	0.75
	$^\dagger 4\ell Z$	862	16.5	2.2	2.1
	$^\dagger 2\ell 2W$	2.74×10^4	639	11.7	1.2

TABLE I. The expected number of signal and background events for the 2ℓ channel at future e^+e^- collider with $\sqrt{s} = 240$ GeV and 5.6 ab^{-1} integrated luminosity. Signal rates assume a benchmark branching fraction $\text{BR}(h_1 \rightarrow NN) = 9.1 \times 10^{-4}$. Background channels marked with † require wrong sign or missing leptons. Non-numeric dashes denote for event numbers below 10^{-3} .

Since t -quark contamination is not a problem in e^+e^- collision, b -jet veto is not included; τ veto is still helpful in removing multi- τ background events. The expected number of events at different cut stages for signal and background channels are listed in Table I. The benchmark branching fraction $\text{BR}(h_1 \rightarrow NN)$ is chosen to be 9.1×10^{-4} , so that the pre-cut (‘initial’) signal event rate is around 10^3 and the signal cut efficiencies can be conveniently converted. The expected signal event number N_s with selection cuts can be calculated from Eq. 4.

The major background includes $4\ell Z$, $2\tau Z$, $2\ell 2\tau Z$ and $2\ell 2W$ channels. The $4\ell Z$ and $2\ell 2\tau Z$ channels can fake a signal by missing two final state leptons with the same sign. In the $2\ell 2W$ channel, $W \rightarrow jj$ provides the required jets, and one missed lepton with the opposite sign can result in a fake signal event. As shown in Table I, these channels contribute more background events than the ‘intrinsic’ $4\tau Z$ channel, and it shows the complication with selecting only one pair of same-sign leptons. The $2\tau Z$ background events are likely from one wrong-sign lepton.

IV. THREE LEPTON CHANNEL

When one N decays leptonically and the other N decays semileptonically, the three leptons in the final state $Zh_1 \rightarrow \ell^\pm \ell^\pm \ell + 4j + \cancel{E}_T$ may contain one SSSF dilepton combination. Compared to the 2ℓ channel, the SSSF dilepton signal occurs with both lepton number violating ($\Delta L = 2$) and conserving ($\Delta L = 0$) decays of NN . The $\Delta L = 2$ process is shown in Fig. 1. When N couples to at least two lepton flavors (e.g. to both e and μ), The $\Delta L = 0$ process can also obtain the same-sign lepton

from the secondary leptonic $W^* \rightarrow \ell\nu$ vertex instead of the primary $N \rightarrow \ell W$ vertex. Therefore, both the Dirac and Majorana N can contribute to this signal.

Similar to the 2ℓ channel, the SM background includes channels with multiple τ and W bosons. The OSSF lepton pair (e.g. $e^\pm e^\mp$) should be vetoed to suppress the SM background.

We select signal events with the following cuts:

- (i) exactly three leptons $N(\ell) = 3$ with $p_T \geq 5$ GeV;
- (ii) veto OSSF lepton pairs;
- (iii) veto τ leptons, $N(\tau) = 0$;
- (iv) at least two jets, $N(j) \geq 2$.

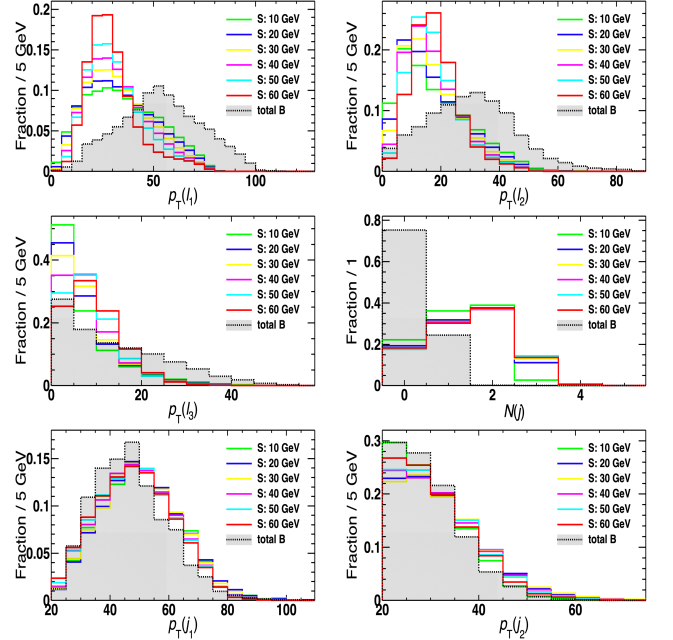


FIG. 3. Normalized distribution of selected kinematic variables for the 3ℓ channel. $p_T(\ell)$ panels are after selecting $N(\ell) = 3$; $N(j)$ is after cut (ii); $p_T(j_1), p_T(j_2)$ are after requiring cuts(i-iv). $N(j)$ cut is selected to optimize the signal significance.

The distributions of selected kinetic variables in the 3ℓ channel are shown in Fig. 3. $p_T(\ell_1), p_T(\ell_2), p_T(\ell_3)$ correspond to the samples after requiring $N(\ell) = 3$; $N(j)$ is after selecting cuts(i-ii); $p_T(j_1), p_T(j_2)$ are after requiring cuts(i-iv). $N(j)$ cut is selected to optimize the signal significance.

Table II lists the expected number of events at different cut stages for signal with different N masses and background channels. In clear contrast to the 2ℓ channel, the surviving backgrounds are $2\tau 2W$ and $2\tau 2\ell Z$ channels. The combination of $N(j)$ cut and increased lepton number cut effectively remove the contamination from leptonic W decays, which leads to a smaller total background event rate. Because of both a lower leptonic N decay branching fraction and fewer jets from NN decays, the signal event rate is also lower compared to the 2ℓ channel.

Interestingly, selecting three leptons will pick up a

		initial	cuts(i)	cuts(ii)	cuts(iii-iv)
Sig.	10 GeV	10^3	27.9	5.6	2.3
	20 GeV	10^3	62.7	13.6	6.6
	30 GeV	10^3	85.8	19.9	10.0
	40 GeV	10^3	102	24.9	12.7
	50 GeV	10^3	112	27.3	14.1
	60 GeV	10^3	115	28.2	14.4
Bkg.	4τ	1.69×10^4	614	155	3.8×10^{-2}
	$^\dagger 2\tau Z$	6.80×10^5	1.30×10^4	350	-
	$^\dagger 2\ell Z$	1.74×10^6	5.03×10^4	121	-
	$4\tau Z$	93.0	2.1	0.25	7.3×10^{-2}
	$2\tau 2W$	4.42×10^3	27.8	6.9	0.72
	$^\dagger 2\ell 2\tau Z$	584	46.5	1.1	0.44
	$^\dagger 4\ell Z$	862	132	0.27	1.4×10^{-2}
	$^\dagger 2\ell 2W$	2.74×10^4	1.30×10^3	37.8	5.0×10^{-2}

TABLE II. Similar to Table I but for the 3ℓ channel. Background channels with † require missing leptons.

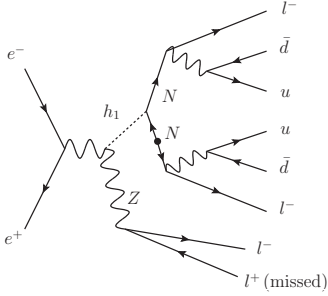


FIG. 4. SS triplepton emerges when Z decay leptonically and the oppose-sign lepton misses detection.

same-sign *trilepton* final state of $\ell^\pm \ell^\pm \ell^\pm$ that derives from leptonic Z decay, as shown in Fig. 4. The jets from semileptonic NN decay satisfy the jet cuts, $\ell^\pm \ell^\pm \ell^\pm$ emerges once the opposite-sign ℓ^\mp misses detection. Among $\ell^\pm \ell^\pm \ell^\pm$ events, about 25% have the same flavor for all three leptons (i.e. SSSF tripleton $e^\pm e^\pm e^\pm$ and $\mu^\pm \mu^\pm \mu^\pm$). When $m_N = 60$ GeV, this $\ell^\pm \ell^\pm \ell^\pm$ final state is 7.6% of the $\ell^\pm \ell^\pm \ell^\pm$ signal events after selecting cuts(i-ii). In comparison, SM events would need at least three missed or wrong-sign leptons to fake such a process. The SSSF tripleton background rate is found to be about 0.1% of the original 3ℓ background event rate after cut (ii). If capped by luminosity limits, SSSF tripleton signal doesn't necessarily yield stronger sensitivity as its expected signal event rate is small.

V. FOUR LEPTON CHANNEL

The fully leptonic NN decay leads to four charged leptons. When N couples to both the first and second lepton generations, two SSSF dileptons $e^\pm e^\pm \mu^\mp \mu^\mp$ can emerge, and the two pairs must be in different flavors to avoid the OSSF dilepton pairs. Due to the presence of

(anti)neutrinos, this final state does not guarantee LNV, and receives contribution from both LNV and non-LNV decays of N . Therefore, both the Dirac and Majorana N can contribute to this signal.

The fully-leptonic branching fraction is lower than the semileptonic branching fraction due to the smaller leptonic $W^* \rightarrow l\nu$ branching compared to the hadronic $W^* \rightarrow jj$ branching, plus the requirement that the two dileptons must differ in flavor. Having two SSSF dileptons can provide *major* reduction on backgrounds, and it is shown that the SM background can be below single-event level in pp collision [25]. At e^+e^- collision, even lower background is expected, and it would be interesting to investigate at what luminosity level the background becomes relevant.

Similar to the semileptonic case, the SM background arise from multiple τ, W channels with one associated Z boson. We consider the following selection cuts in event analysis:

- (i) exactly four leptons, $N(\ell) = 4$ with $p_T(\ell) \geq 5$ GeV;
- (ii) exactly two electrons with the same charges; exactly two muons with the same charges; electrons and muons have opposite charges; i.e. exactly $e^\pm e^\pm \mu^\mp \mu^\mp$ lepton pairs;
- (iii) veto τ leptons, $N(\tau) = 0$;
- (iv) at least one jet, $N(j) \geq 1$.

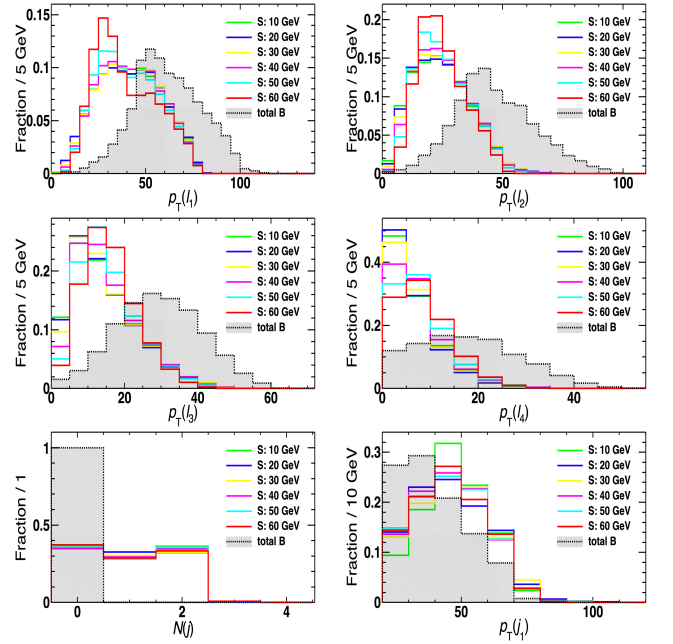


FIG. 5. Normalized distribution of selected kinematic variables for the 4ℓ channel. $p_T(\ell)$ panels are after selecting $N(\ell) = 4$, $N(j)$ is after cut (ii), $p_T(j)$ panels are after cut (iv).

The kinetic distributions of selected observables for the signal with different N masses and the total background are shown in Fig. 5. $p_T(\ell_1)$, $p_T(\ell_2)$, $p_T(\ell_3)$, $p_T(\ell_4)$ correspond to the samples after requiring $N(\ell) = 4$; $N(j)$ is

after selecting cuts(i-ii); $p_T(j_1)$ is after requiring cuts(i-iv).

		initial	cuts(i)	cuts(ii)	cuts(iii-iv)
Sig.	10 GeV	10^3	15.9	1.1	0.71
	20 GeV	10^3	17.5	1.1	0.72
	30 GeV	10^3	22.1	1.3	0.80
	40 GeV	10^3	26.8	1.5	0.98
	50 GeV	10^3	30.1	1.8	1.2
	60 GeV	10^3	32.1	2.1	1.3
Bkg.	4τ	1.69×10^4	58.4	6.8	-
	$^\dagger 2\tau Z$	6.80×10^5	2.26×10^3	9.6	-
	$^\dagger 2\ell Z$	1.74×10^6	7.28×10^4	-	-
	$4\tau Z$	93.0	0.45	6.4×10^{-3}	2.8×10^{-3}
	$2\tau 2W$	4.42×10^3	1.3	0.17	-
	$^\dagger 2\ell 2\tau Z$	584	13.8	1.0×10^{-2}	3.2×10^{-3}
	$^\dagger 4\ell Z$	862	116	7.8×10^{-4}	-
	$^\dagger 2\ell 2W$	2.74×10^4	217	-	-

TABLE III. Similar to Table I but for the 4ℓ channel. Background channels with † require missing leptons or wrong signs.

The expected number of events at different cut stages for signal with different N masses and background channels are shown in Table III. Due to two SSSF dileptons, two wrong-sign leptons must occur to fake such an event. Missing leptons are also less a problem as it would take a $2\tau 2e 2\mu Z$ final state with one missed e and one missed μ to fake the signal.

The surviving backgrounds are the $4\tau Z$ and $2\ell 2\tau Z$ channels. The lepton flavor and opposite-sign cuts play the central role in rejecting the background with same flavor, oppose-sign leptons. Stringent lepton counting removes the contamination from hadronic τ decays. The $2\tau 2\ell Z$ channel still contributes to background events, possibly due to wrong sign leptons.

VI. RESULTS

Signal event samples are generated with the $e^+e^- \rightarrow ZNN$ process and then we let Z boson and the right-hand neutrinos decay inclusively. The signal event rate is,

$$N_s = L \cdot \sigma_{Zh_1} \cdot \text{BR}(h_1 \rightarrow NN) \cdot \eta_s \quad (4)$$

where L is the collider luminosity and η_s denotes the cut-based selection efficiency on the generated signal events. With a design luminosity $L = 5.6 \text{ ab}^{-1}$ and $\sigma_{Zh_1} = 196 \text{ fb}$ at 240 GeV center-of-mass energy [16], a sample of 1.1×10^6 Zh_1 events are expected. Since we let N decay inclusively, η_s already includes the NN system's combined branching fraction into the selected final states, thus the formula above does not explicitly contain the N decay branching fraction. The signal's statistic significance is

$$\sigma_{\text{stat}} = \sqrt{2[(N_s + N_b)\ln(1 + \frac{N_s}{N_b}) - N_s]}. \quad (5)$$

The background event rates N_b for 2ℓ , 3ℓ and 4ℓ channels are listed in Table I, II and III, respectively. Requiring 2σ and 5σ significance levels, the sensitivity limits on $\text{BR}(h_1 \rightarrow NN)$ are shown in Fig. 6.

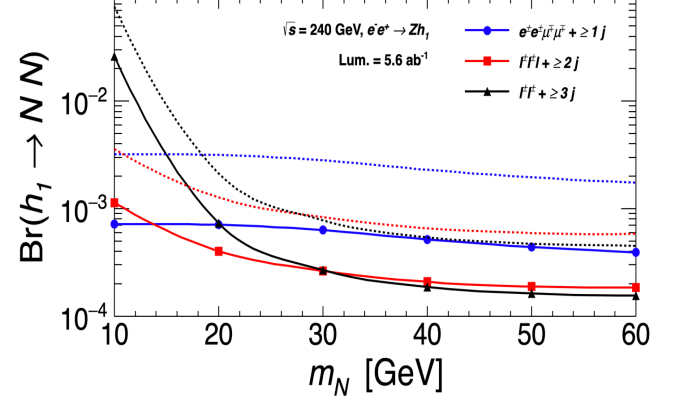


FIG. 6. Sensitivity limits on the decay branching ratio of Higgs boson to NN for $2\text{-}4\ell$ channels assuming m_N between 10 and 60 GeV. Zh_1 production assumes 240 GeV center-of-mass energy and 5.6 ab^{-1} integrated luminosity at future e^-e^+ colliders. The solid (dotted) curves correspond to $2\sigma(5\sigma)$ significance.

Given $L \cdot \sigma_{Zh_1} \sim 10^6$, the $\text{BR}(h_1 \rightarrow NN)\eta_s$ combination in Eq. 4 is statistically limited by $N_s/N_{Zh_1} \sim 10^{-6}N_s$. The selection efficiency η_s is favorably evaluated via Monte Carlo, as η_s is weighted between different decay chains that contribute to the same final state. In our case, both $Z \rightarrow \ell\ell, jj$ contribute to the signal channels.

Note 2ℓ and 3ℓ limits worsen towards lower m_N . This is caused by N decaying into collimated leptons and jets when N becomes more boosted at smaller m_N , resulting in fewer reconstructed jets, hence hard hit by the $N(j)$ cut. Relaxing the jet counting cut would help recovering more low m_N signal events, yet at the cost of significantly increasing the SM background. The 4ℓ channel has the highest background veto efficiency that can saturate luminosity cap ($N_b < 1$) up to 10^3 ab^{-1} . Due to sub-unity background event rate, the 4ℓ channel's sensitivity is less stringent than 2ℓ and 3ℓ channels because of its much lower signal selection efficiency.

$\text{BR}(h_1 \rightarrow NN)$ relates to BSM parameters as

$$|\sin \alpha \cdot y_S|^2 = \text{BR}(h_1 \rightarrow NN) \quad (6)$$

$$\times \epsilon \cdot 16\pi \frac{\Gamma_{h_1}}{m_{h_1}} \left(1 - \frac{4m_N^2}{m_{h_1}^2}\right)^{-3/2},$$

where $\epsilon = 1$ for Majorana N and $\epsilon = 1/2$ for Dirac N . With the total Higgs boson width $\Gamma_{h_1} \sim 4 \text{ MeV}$, a $\text{BR}(h_1 \rightarrow NN) = 10^{-4}$ sensitivity limit would correspond to $|\sin \alpha \cdot y_S|^2 \leq 7.3 \times 10^{-6}$ at $m_N = 60 \text{ GeV}$, or $\leq 1.6 \times 10^{-7}$ towards low N mass $2m_N \ll m_{h_1}$ where the decay phase space is unsuppressed. y_S is a free model parameter given by v_S and m_N . For $y_S \sim \mathcal{O}(1)$, this

limit constrains $|\sin \alpha|$ to be lower than 10^{-2} . This shows that the future Higgs factory has good sensitivity to tiny effective mixing angles between the Higgs boson and the BSM singlet scalar, which is comparable to the projected $|\sin \alpha|^2 \sim 10^{-4}$ sensitivity at the LHC [25].

Acknowledgments

Y.G. is supported by the Institute of High En-

ergy Physics, Chinese Academy of Sciences under the CEPC theory grant (2019-2020) and partially under grant no. Y7515560U1. K.W. is supported by the National Natural Science Foundation of China under grant no. 11905162, the Excellent Young Talents Program of the Wuhan University of Technology under grant no. 40122102, the research program of the Wuhan University of Technology under grant no. 3120620265, and the CEPC theory grant (2019-2020) of the Institute of High Energy Physics, Chinese Academy of Sciences.

-
- [1] Peter Minkowski, “ $\mu \rightarrow e\gamma$ at a Rate of One Out of 10^9 Muon Decays?” *Phys. Lett.* **67B**, 421–428 (1977).
 - [2] Tsutomu Yanagida, “Horizontal gauge symmetry and masses of neutrinos, Proceedings: Workshop on the Unified Theories and the Baryon Number in the Universe,” *Tsukuba, Japan, February 13-14, 1979*, *Conf. Proc.* **C7902131**, 95–99 (1979).
 - [3] Rabindra N. Mohapatra and Goran Senjanovic, “Neutrino Mass and Spontaneous Parity Nonconservation,” *Phys. Rev. Lett.* **44**, 912 (1980).
 - [4] S. L. Glashow, “The Future of Elementary Particle Physics,” *Cargese Summer Institute, 1979*, *NATO Sci. Ser. B* **61**, 687 (1980).
 - [5] Murray Gell-Mann, Pierre Ramond, and Richard Slansky, “Complex Spinors and Unified Theories,” *Supergravity Workshop, 1979*, *Conf. Proc.* **C790927**, 315–321 (1979).
 - [6] Anupama Atré, Tao Han, Silvia Pascoli, and Bin Zhang, “The Search for Heavy Majorana Neutrinos,” *JHEP* **05**, 030 (2009), arXiv:0901.3589 [hep-ph].
 - [7] Albert M Sirunyan et al. (CMS), “Search for heavy neutral leptons in events with three charged leptons in proton-proton collisions at $\sqrt{s} = 13$ TeV,” *Phys. Rev. Lett.* **120**, 221801 (2018), arXiv:1802.02965 [hep-ex].
 - [8] Georges Aad et al. (ATLAS), “Search for heavy neutral leptons in decays of W bosons produced in 13 TeV pp collisions using prompt and displaced signatures with the ATLAS detector,” *JHEP* **10**, 265 (2019), arXiv:1905.09787 [hep-ex].
 - [9] Roel Aaij et al. (LHCb), “Search for heavy neutral leptons in $W^+ \rightarrow \mu^+ \mu^\pm \text{jet}$ decays,” (2020), arXiv:2011.05263 [hep-ex].
 - [10] Albert M Sirunyan et al. (CMS), “Search for high-mass resonances in dilepton final states in proton-proton collisions at $\sqrt{s} = 13$ TeV,” *JHEP* **06**, 120 (2018), arXiv:1803.06292 [hep-ex].
 - [11] Georges Aad et al. (ATLAS), “Search for new resonances in mass distributions of jet pairs using 139 fb^{-1} of pp collisions at $\sqrt{s} = 13$ TeV with the ATLAS detector,” *JHEP* **03**, 145 (2020), arXiv:1910.08447 [hep-ex].
 - [12] Paul Langacker, “The Physics of Heavy Z' Gauge Bosons,” *Rev. Mod. Phys.* **81**, 1199–1228 (2009), arXiv:0801.1345 [hep-ph].
 - [13] E. Akhmedov, A. Kartavtsev, M. Lindner, L. Michaels, and J. Smirnov, “Improving Electro-Weak Fits with TeV-scale Sterile Neutrinos,” *JHEP* **05**, 081 (2013), arXiv:1302.1872 [hep-ph].
 - [14] Luca Di Luzio, Ramona Gröber, and Michael Spannowsky, “Maxi-sizing the trilinear Higgs self-coupling: how large could it be?” *Eur. Phys. J. C* **77**, 788 (2017), arXiv:1704.02311 [hep-ph].
 - [15] J. Alison et al., “Higgs boson potential at colliders: Status and perspectives,” *Rev. Phys.* **5**, 100045 (2020), arXiv:1910.00012 [hep-ph].
 - [16] Mingyi Dong et al. (CEPC Study Group), “CEPC Conceptual Design Report: Volume 2 - Physics & Detector,” (2018), arXiv:1811.10545 [hep-ex].
 - [17] D. Wyler and L. Wolfenstein, “Massless Neutrinos in Left-Right Symmetric Models,” *Nucl. Phys.* **B218**, 205–214 (1983).
 - [18] Pierre Fayet, “Supergauge Invariant Extension of the Higgs Mechanism and a Model for the electron and Its Neutrino,” *Nucl. Phys. B* **90**, 104–124 (1975).
 - [19] Daniele Barducci, Enrico Bertuzzo, Andrea Caputo, Pilar Hernandez, and Barbara Mele, “The see-saw portal at future Higgs Factories,” (2020), arXiv:2011.04725 [hep-ph].
 - [20] K. Belotsky, Daniele Fargion, M. Khlopov, R. Konoplich, and K. Shibaev, “Invisible Higgs boson decay into massive neutrinos of fourth generation,” *Phys. Rev. D* **68**, 054027 (2003), arXiv:hep-ph/0210153.
 - [21] Ian M. Shoemaker, Kalliopi Petraki, and Alexander Kusenko, “Collider signatures of sterile neutrinos in models with a gauge-singlet Higgs,” *JHEP* **09**, 060 (2010), arXiv:1006.5458 [hep-ph].
 - [22] Alessio Maiezza, Miha Nemevšek, and Fabrizio Nesti, “Lepton Number Violation in Higgs Decay at LHC,” *Phys. Rev. Lett.* **115**, 081802 (2015), arXiv:1503.06834 [hep-ph].
 - [23] Miha Nemevšek, Fabrizio Nesti, and Juan Carlos Vasquez, “Majorana Higgses at colliders,” *JHEP* **04**, 114 (2017), arXiv:1612.06840 [hep-ph].
 - [24] S. Moretti, C. H. Shepherd-Themistocleous, and H. Waktari, “Lepton number violation in heavy Higgs boson decays to sneutrinos,” *Phys. Rev. D* **101**, 015018 (2020), arXiv:1909.04692 [hep-ph].
 - [25] Yu Gao, Mingjie Jin, and Kechen Wang, “Probing the Decoupled Seesaw Scalar in Rare Higgs Decay,” *JHEP* **02**, 101 (2020), arXiv:1904.12325 [hep-ph].
 - [26] “CEPC Conceptual Design Report: Volume 1 - Accelerator,” (2018), arXiv:1809.00285 [physics.acc-ph].
 - [27] “The International Linear Collider Technical Design Report - Volume 2: Physics,” (2013), arXiv:1306.6352 [hep-ph].
 - [28] A. Abada et al. (FCC), “FCC-ee: The Lepton Collider: Future Circular Collider Conceptual Design Report Volume 2,” *Eur. Phys. J. ST* **228**, 261–623 (2019).
 - [29] Albert M Sirunyan et al. (CMS), “Search for a standard

- model-like Higgs boson in the mass range between 70 and 110 GeV in the diphoton final state in proton-proton collisions at $\sqrt{s} = 8$ and 13 TeV,” *Phys. Lett. B* **793**, 320–347 (2019), arXiv:1811.08459 [hep-ex].
- [30] Vardan Khachatryan et al. (CMS), “Search for diphoton resonances in the mass range from 150 to 850 GeV in pp collisions at $\sqrt{s} = 8$ TeV,” *Phys. Lett. B* **750**, 494–519 (2015), arXiv:1506.02301 [hep-ex].
 - [31] Arindam Das, Yu Gao, and Teruki Kamon, “Heavy Neutrino Search via the Higgs boson at the LHC,” (2017), arXiv:1704.00881 [hep-ph].
 - [32] Shankha Banerjee, P. S. Bhupal Dev, Alejandro Ibarra, Tanumoy Mandal, and Manimala Mitra, “Prospects of Heavy Neutrino Searches at Future Lepton Colliders,” *Phys. Rev. D* **92**, 075002 (2015), arXiv:1503.05491 [hep-ph].
 - [33] Arindam Das, P. S. Bhupal Dev, and C. S. Kim, “Constraining Sterile Neutrinos from Precision Higgs Data,” *Phys. Rev. D* **95**, 115013 (2017), arXiv:1704.00880 [hep-ph].
 - [34] Jian-Nan Ding, Qin Qin, and Fu-Sheng Yu, “Heavy neutrino searches at future Z -factories,” *Eur. Phys. J. C* **79**, 766 (2019), arXiv:1903.02570 [hep-ph].
 - [35] Zeren Simon Wang and Kechen Wang, “Physics with far detectors at future lepton colliders,” *Phys. Rev. D* **101**, 075046 (2020), arXiv:1911.06576 [hep-ph].
 - [36] J. Alwall, R. Frederix, S. Frixione, V. Hirschi, F. Maltoni, O. Mattelaer, H. S. Shao, T. Stelzer, P. Torrielli, and M. Zaro, “The automated computation of tree-level and next-to-leading order differential cross sections, and their matching to parton shower simulations,” *JHEP* **07**, 079 (2014), arXiv:1405.0301 [hep-ph].
 - [37] Torbjorn Sjostrand, Stephen Mrenna, and Peter Z. Skands, “PYTHIA 6.4 Physics and Manual,” *JHEP* **05**, 026 (2006), arXiv:hep-ph/0603175.
 - [38] Torbjorn Sjostrand, Stephen Mrenna, and Peter Z. Skands, “A Brief Introduction to PYTHIA 8.1,” *Comput. Phys. Commun.* **178**, 852–867 (2008), arXiv:0710.3820 [hep-ph].
 - [39] S. Jadach, Z. Was, R. Decker, and Johann H. Kuhn, “The tau decay library TAUOLA: Version 2.4,” *Comput. Phys. Commun.* **76**, 361–380 (1993).
 - [40] J. de Favereau, C. Delaere, P. Demin, A. Giammanco, V. Lemaitre, A. Mertens, and M. Selvaggi (DELPHES 3), “DELPHES 3, A modular framework for fast simulation of a generic collider experiment,” *JHEP* **02**, 057 (2014), arXiv:1307.6346 [hep-ex].
 - [41] Cheng Chen, Xin Mo, Michele Selvaggi, Qiang Li, Gang Li, Manqi Ruan, and Xinchou Lou, “Fast simulation of the CEPC detector with Delphes,” (2017), arXiv:1712.09517 [hep-ex].
 - [42] Claudio O. Dib, C. S. Kim, and Kechen Wang, “Signatures of Dirac and Majorana sterile neutrinos in trilepton events at the LHC,” *Phys. Rev. D* **95**, 115020 (2017), arXiv:1703.01934 [hep-ph].
 - [43] Stefan Antusch, Eros Cazzato, Oliver Fischer, A. Hammad, and Kechen Wang, “Lepton Flavor Violating Dilepton Dijet Signatures from Sterile Neutrinos at Proton Colliders,” *JHEP* **10**, 067 (2018), arXiv:1805.11400 [hep-ph].